The vertical structure of CO in the Martian atmosphere from the ExoMars Trace Gas Orbiter

Kevin Olsen, Franck Lefèvre, Franck Montmessin, A. A. Fedorova, A. Trokhimovskiy, Lucio Baggio, Oleg Korablev, J. Alday, C. Wilson, Francois, Forget, et al.

The vertical structure of CO in the Martian atmosphere from the ExoMars Trace Gas Orbiter

K. S. Olsen[1,2✉], F. Lefèvre[2], F. Montmessin[2], A. A. Fedorova[3], A. Trokhimovskiy[3]

L. Baggio[2], O. Korablev[3], J. Alday[1], C. F. Wilson[1], F. Forget[4], D. A. Belyaev[3],

A. Patrakeev[3], A. V. Grigoriev[3], and A. Shakun[3]

[1] Department of Physics, University of Oxford, Oxford, UK,

[2] Laboratoire Atmosphères, Milieux, Observations Spatiales (LATMOS),

Université Paris-Saclay, Sorbonne Université,

Centre National de la Recherche Scientifique (CNRS),Guyancourt, France,

[3] Space Research Institute of the Russian Academy of Sciences (IKI RAS), Moscow, Russia

[4] Laboratoire de Météorologie Dynamique (LMD), Sorbonne Université, CNRS, Paris, France,

✉e-mail: Kevin.Olsen@physics.ox.ac.uk

November 11, 2020

Abstract

Carbon monoxide (CO) is the main product of CO_2 photolysis in the Martian atmosphere. Production of CO is balanced by its loss reaction with OH, which recycles CO into CO_2. CO is therefore a sensitive tracer of the OH-catalyzed chemistry that contributes to the stability of CO_2 in the atmosphere of Mars. To date, CO has only

been measured in terms of vertically-integrated column abundances and the upper atmosphere, where CO is produced, is largely unconstrained by observations. Here we report vertical profiles of CO from 10 to 120 km, and from a broad range of latitudes, inferred from the Atmospheric Chemistry Suite onboard the ExoMars Trace Gas Orbiter. At solar longitudes 164–190°, we observe an equatorial CO mixing ratio of $\sim$ 1000 ppmv (10–80 km), increasing towards the polar regions to more than 3000 ppmv under the influence of downward transport of CO from the upper atmosphere, providing a view of the Hadley cell circulation at Mars equinox. Observations also cover the 2018 global dust storm, during which we observe a prominent depletion in the CO mixing ratio up to 100 km. This is indicative of increased CO oxidation in a context of unusually large high-altitude water vapour, boosting OH abundance.

Carbon monoxide (CO) plays an important part in the Martian atmosphere, with an integral role in both hydrogen and oxygen chemical cycles. It is mainly governed by simple chemistry, being produced in the upper atmosphere (60 km) by CO_2 photolysis, and destroyed in the lower atmosphere by the hydroxyl (OH) radical, a product of water vapour (H_2O) photolysis [1, 2, 3, 4, 5]. Tracking atmospheric CO on Mars is an effective method for exploring the oxidizing capacity of the Martian atmosphere. The abundance of CO reflects the rate at which CO_2 is recycled by the catalytic HO_x chemical cycles, addressing the fundamental issue of the long-term stability of Mars' atmospheric composition. The quantitative understanding of CO has remained a challenge: most theoretical models predict a long-term equilibrium value for the CO volume mixing ratio (VMR) that is smaller by a factor 2–4 than those observed [5]. The persistence of this disagreement suggests that an important part of our understanding of Martian atmospheric chemistry remains missing.

Past observations of CO below the thermosphere have been limited to vertically integrated column abundances, and published abundances are representative of the denser, lower atmosphere. These measurements indicate a slow seasonal variation of CO imparted by the global

CO_2 condensation-sublimation cycle (e.g., [6]). The lifetime of CO is ~ 5 terrestrial years, so such a seasonal cycle is expected [6]. Recent satellite observations made with instruments on Mars Express (MEx) and Mars Reconnaissance Orbiter (MRO) have observed CO volume mixing ratios of between 500–1000 ppmv [7, 8, 9, 10]. Variations are more pronounced in polar regions where the CO VMR is directly affected by near-surface CO_2 sublimation and condensation, as is argon [11, 12]. The most extensive coverage comes from the Compact Reconnaissance Imaging Spectrometer (CRISM) [13, 10], which found a mean mixing ratio at mid-latitudes of around 800 ppmv, with a seasonal low-latitude enhancements reaching about 1000 ppmv around solar longitude (Ls) of 180°.

Observations of vertical changes to CO density have been made *in situ* by the Neutral Gas and Ion Mass Spectrometer (NGIMS) on the Mars Atmosphere and Volatile Evolution (MAVEN) satellite [14]. These measurements are of the particle flux of neutral CO molecules collected between 140–350 km during low-altitude MAVEN orbits. The density measurements are restricted to the thermosphere and ionosphere, and full mixing ratio vertical profiles have not been produced. CO^+ ions have also been detected [15].

Using the Atmospheric Chemistry Suite (ACS) mid-infrared channel (MIR) onboard the ExoMars Trace Gas Orbiter (TGO), we present the first vertical profiles of CO in the Martian atmosphere. These measurements obtained with the solar occultation technique give access for the first time to the production region of CO in the upper atmosphere (above 60 km), putting strong constraints on the CO formation rate or, equivalently, the CO_2 photolysis rate, since there is negligible accompanying CO loss at high altitudes. Above the poles, ACS measurements of CO characterize the equator-to-pole Hadley circulation that transports CO from its extra-polar region of production, revealing the pole-ward fluxes of atmospheric mass involved. Our measurements also cover the particular conditions of the Mars year (MY) 34 global dust storm, supplying direct information on the impact of such events on chemistry atmospheric circulation, particularly at high altitudes.

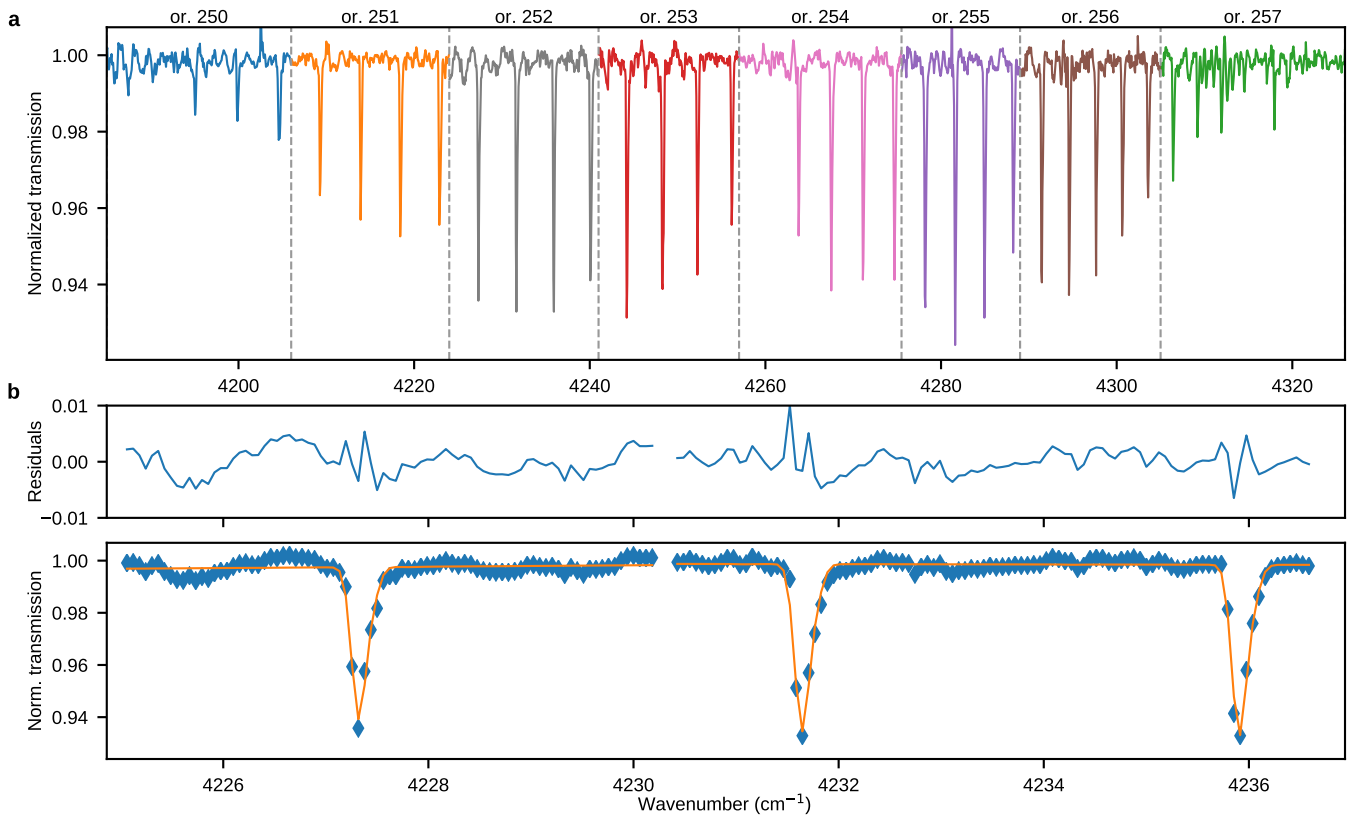

Fig. 1. | **Spectral fitting with ACS MIR** Example of normalized spectra recorded at 60 km with ACS MIR using secondary grating position 7. Shown are: (a) contributions from diffraction orders 250–257, (b) example fits for spectral windows covering order 252 (bottom) and the associated residuals (top).

Fig. 1a shows an example spectrum from a single occultation at 60 km featuring the 2-0 band of CO. Fig. 1b shows the fit for one order and the associated residuals. Details about the ACS MIR instrument, data processing, and VMR vertical profile retrievals are provided in Supplementary Methods and Supplementary Figs. 1–3. Vertical profiles of T and P were retrieved from simultaneous observations made by the near-infrared (NIR) channel of ACS [16, 17]. Details about NIR are given in the Supplementary Methods, as are vertical profiles of the CO volume mixing ratio, T, and P that were generated by running the LMD general circulation model (GCM) [18, 19] at coincident times and locations using a reconstructed dust climatology for MY 34 [20] (see Supplementary Methods and Supplementary Figs. 4–5

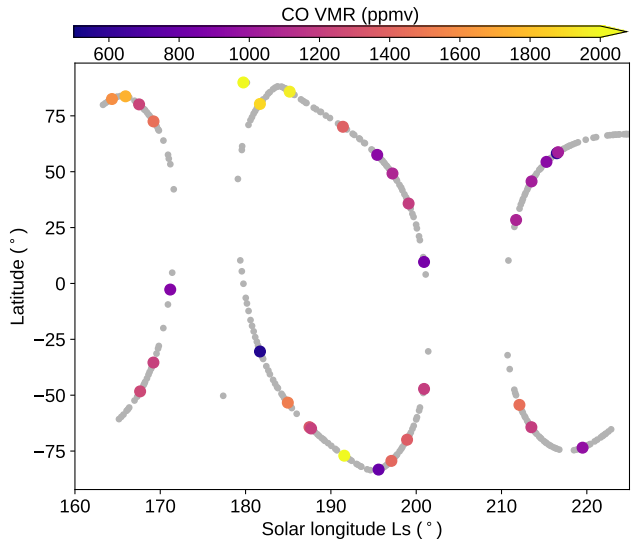

Fig. 2. | **Solar occultation latitudes** Distribution over latitude and solar longitude of ACS MIR occultation using position 7, and all other ACS occultation points. The colour scale indicates the retrieved CO VMR between 20–40 km. The solar longitudes correspond to an observational period of April to September 2018.

ACS MIR was used in a configuration suitable for CO retrievals (with secondary grating position 7) for only a small fraction of observations. Herein we present analysis of the first 32 occultations recorded between Ls 164° and 220° (April 24 2018 and June 28 2018). The latitudinal distribution of these observations is shown in Fig. 2 as a function of solar longitude. Fig. 2 also indicates the mean VMR of CO between 20–40 km, and the distribution of all other ACS MIR occultations. A list of location and time information for these observations is given in Supplementary Table 1.

Mid-latitude observations

The first set of CO retrievals we present were measured at mid-to-low latitudes around the northern hemisphere autumnal equinox, prior to Ls 190°. Previous measurements of the CO vertical column indicate that this is a period when the CO outside the polar regions is largest [21, 10]. Fig. 3a presents the retrieved vertical profiles of the CO mixing ratio from

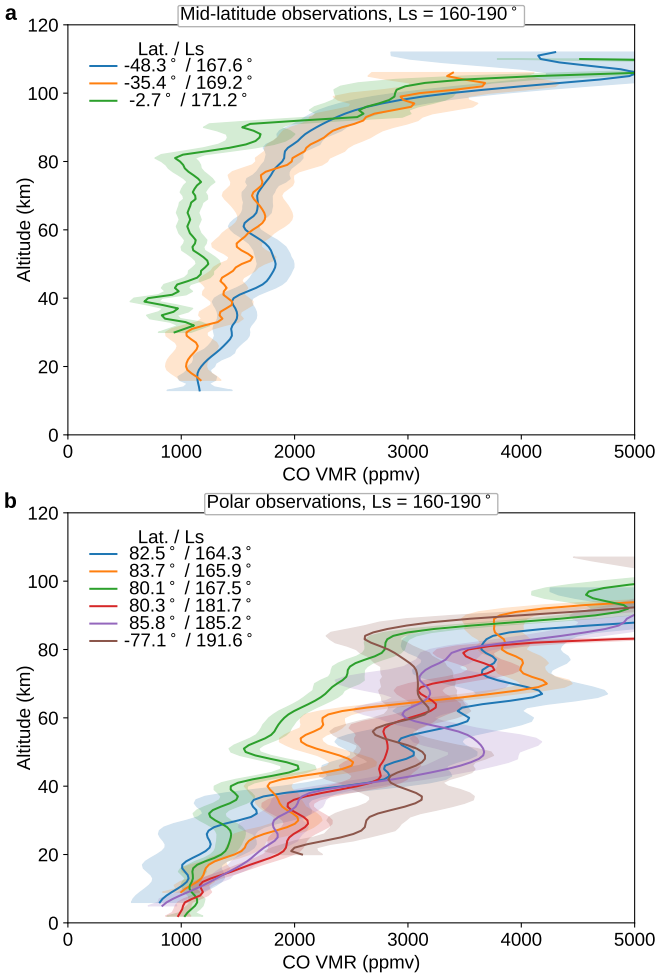

Fig. 3. | CO VMR vertical profiles at different latitudes Vertical profiles of retrieved CO mixing ratio as observed by ACS MIR at: a) equatorial and mid-latitudes prior to Ls 190°, and b) at polar latitudes greater than ±75°. The shaded areas show the magnitude of the uncertainty of each retrieved VMR value. Lower altitude ranges are limited by signal attenuation due to aerosols. Uncertainties are derived from the non-linear least squaresd inversion using partial derivatives.

ACS measurements outside the polar regions, and prior to the onset of the global dust storm (individual retrievals are shown in Supplementary Figs. 6–7). The altitudes at which a reliable retrieval can be performed have upper and lower limits caused by signal attenuation due to aerosols that become significant below 30 km, and by the decrease of absorption line depths relative to noise above 100 km.

The north-most ACS MIR observation, made equatorially at −2.7° is about 1000 ppmv,

in good agreement with the CRISM observations. The more southern observations are still impacted by the south polar winter CO enrichment, which is also observed by CRISM [10, 22], and the mean CO mixing ratio rises towards 1260 ppmv. Since the CO mixing ratios are expected to be nearly constant at lower altitudes, this should be comparable to column-averaged abundances. The mean mid-latitude value reported by CRISM during this period is 900–1000 ppmv [10], by PFS is 500–1500 ppmv, and by terrestrial observations is 850–1100 ppmv [21].

The neutral CO densities reported by the NGIMS team approach 10^{10} cm^{-3} at the lowest altitude limits of around 130 km. CO number densities computed from the ACS MIR retrievals and the LMD GCM are in broad agreement at 120 km, covering a range of 10^{9}–10^{10} cm^{-3}. Thus the ACS MIR observations are in agreement with the NGIMS results, but a direct comparison is made cautiously as the uncertainty of ACS MIR retrievals is very large above 100 km, the NGIMS results are likely only reliable above 160 km, and the difference in altitude coverage will have a very significant impact on composition.

Our initial set of observations occurs at a unique time, around the autumnal equinox. This is a period between polar CO enhancements during the past southern winter and upcoming northern winter. It is characterized by a CO meridional distribution expected to be symmetrical across the Equator, under the influence of the mean meridional circulation dominated by a double Hadley cell structure. Fig. 4 shows the evolution of the CO zonal mean modelled by the LMD GCM with photochemistry [19]. Panel (a) shows a symmetric CO distribution at the start of observations, and panel (b) reveals an oncoming change in the downwelling strength over the polar regions. Around Ls 190°, the Martian atmosphere was severely affected by a global dust storm that began in the southern hemisphere [23, 24], shown in panel (c) and discussed below.

The vertical profiles observed by ACS are fairly uniform up to around 80 km, at which point the mixing ratios begin to increase rapidly due to CO_2 photolysis. This is distinct

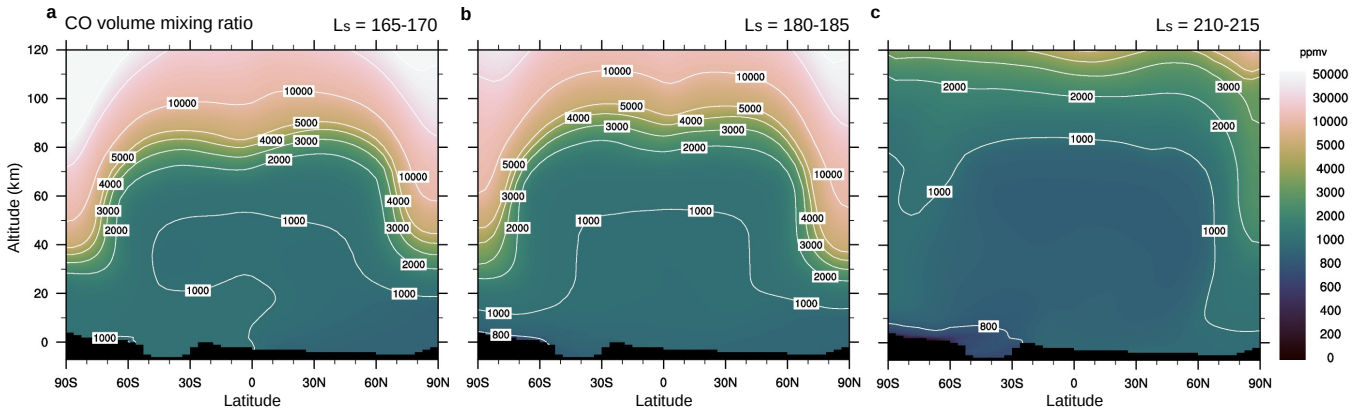

Fig. 4. | **Modelled CO distributions** Zonally-averaged CO volume mixing ratio (ppmv) calculated by the LMD global climate model using the MY 34 dust climatology [20] for three Ls periods: a) 165–170°, b) 180–185°, c) 210–215°. The onset of the global dust storm was around Ls 190°. The simulation shown here was initialized at Ls = 180° of MY33 and therefore avoids known issues with photochemical models underestimating the long-term equilibrium value of CO.

from GCM predictions which have more pronounced mixing ratio increases occurring just above 60 km. This indicates that we are observing stronger upward transport of CO, the equatorial ascending branch of Hadley circulation, than modelled in the GCM. Zonal means at all latitudes derived from the GCM prior to Ls 190° are shown in Fig. 4a and b. This shows a well mixed atmosphere between −50° and 50° with increasing CO abundance pole-ward. CO vertical profiles measured by ACS at southern mid-latitudes show a more distinct increase in CO compared to the equatorial profile. This is likely to be related to the downwelling motion that occurs above both poles around equinox as observed seasonally by CRISM [10]. That it is also more pronounced than in the GCM again suggests a more intense Hadley circulation in the real atmosphere than modelled.

We have found that when using T and P derived by the GCM, rather than ACS NIR retrievals, our retrieved CO VMR tends toward closer agreement with the GCM CO. This implies that any underestimation of the CO mixing ratio by the GCM is also linked to differences in the physical state of the atmosphere between model and observation.

High-latitude observations

Fig. 3b shows the CO VMR vertical profiles retrieved at latitudes greater than 75° in both hemispheres. Close to the surface the CO mixing ratio measured by ACS near the poles remains between 900–1200 ppmv as in mid-to-low latitudes. The increase in CO with altitude is however much more pronounced at high latitudes, where the mixing ratios are of the order of 2000–3000 ppmv at 40 km. Such values are only measured above 80 km at lower latitudes (Fig. 3a). This is a result of the Hadley circulation, which, around equinox, consists in two branches symmetrical across the Equator. Ascending motion prevails at low latitudes, whereas downwelling over both poles brings large quantities of CO produced in the upper atmosphere to the lower atmosphere (see Fig. 4b). During this time period, H_2O VMRs are reduced over both poles, reducing OH availability, but a reduction in CO depletion rates is much smaller than the dynamical changes. The fine structures observed over the altitude range are correlated with those seen in NIR data and are suggestive of horizontal transport, which mixes CO-rich layers coming from the pole with CO-poor air farther from the location of downwelling motion.

While the GCM and retrievals are in qualitative agreement, the rate at which CO increases dramatically over altitude in Fig. 4, and the altitude at which this occurs, are in quantitative disagreement. We see higher mixing ratios than predicted below 40 km, and lower ones above. Such disagreement likely stems from the dynamic model in the GCM. On one hand, the GCM may be over-estimating the strength of polar downwelling. Otherwise, it may be forcing the downwelling over too narrow a latitude range. In the downwelling regions of Fig. 4b, the gradient of the CO vertical profiles changes rapidly with latitude, and GCM results from more southerly latitudes may be more representative of the sampled air masses.

Impact of the global dust storm

From Ls 190° until after Ls 230°, nearly the entire Martian atmosphere was affected by a global dust storm. Fig. 5 shows the evolution of observed vertical profiles over Ls. During this period we observe a strong decrease in the CO VMR over time, as well as increasing vertical transport. The latter is indicated by the rise in the height at which the CO abundance starts to increase. These correspond to the onset of the global dust storm around Ls 190°.

The main impact of a dust event on our ability to study CO is to limit how low in the atmosphere we can probe. As atmospheric density and aerosol loading increase with decreasing altitude, the solar occultation transmission level often falls from unity to zero within 5–10 km (see [16, 17]).

The impacts of the storm on the physical state of the atmosphere and on the water cycle have been studied extensively [e.g., 16, 17, 20]. When dust is lifted into the atmosphere, it absorbs radiation and stores heat. This results in an expansion of the lower layers of the atmosphere, amplified Hadley cell circulation, deep convection, strongly increased water vapour content, and reduced cloud formation. During our period of observation, the hygropause altitude moved from $\sim$ 50 km to between 50–80 km, the VMR of H_2O was enhanced by around 75–150 ppmv [25, 17], and temperature increases on the order of 30–50 K were observed [23].

These impacts due to dust loading are well-reproduced in GCM simulations [e.g., 26], and our own simulations show the resulting changes to CO in Fig. 4c. The zonal mean CO mixing ratio profiles reveal increased Hadley cell circulation: strong upwelling in northern summer as well as at low-to-mid latitudes in the southern winter atmosphere.

If we consider the observations made outside the polar enhancements, we can compute the mean CO mixing ratio below 40 km for the two time periods (before and during the dust storm). After the onset of the dust storm, the mean CO mixing ratio value in our

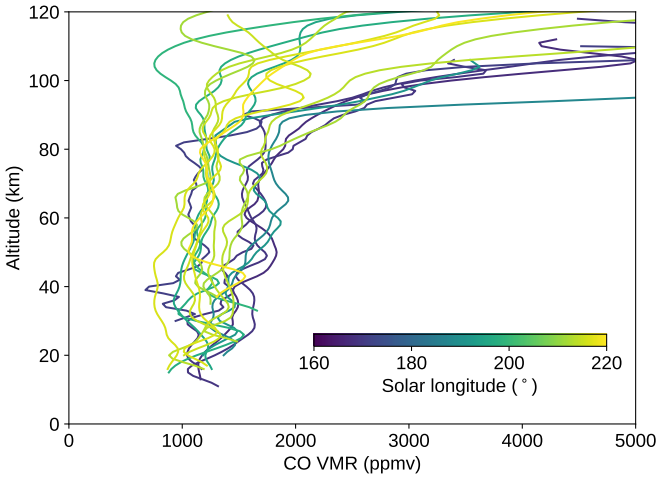

Fig. 5. | Time evolution of CO VMR vertical profiles Evolution of the ACS vertical profiles of CO during the MY34 dust storm. Latitudes are between −75° to 75° and colours indicate Ls.

observations has fallen to 1070 ± 17 ppmv from 1260 ± 30 ppmv, which is greater than a 20% decrease (95% confidence intervals are 1034–1098 ppmv and 1198–1319 ppmv, respectively). These differences are distinctly seen in Fig. 5 and are likely to be due to the large amounts of H_2O present during the dust storm and the subsequent accelerated CO loss by reaction with OH.

At high altitudes, ACS observations of decreased CO mixing ratios after the onset of the global dust storm is explained by the same expansion that raised the hygropause level. Intense warming and increased pressure produce an upward motion that leads to intensified circulation, consistent with our GCM results (Fig. 4). The dramatic increase in the hygropause altitude also increases the vertical range over which OH becomes available to convert CO into CO_2. After the dust storm, we observe CO VMRs that are fairly constant until above 100 km, much higher than observations prior to the dust storm and GCM predictions. This suggests strong vertical mixing, and that the altitude at which the CO_2 mixing ratios are assumed to begin to drop off is elevated.

CO is a tracer for upper atmosphere transport and its quantification is also important

for understanding the oxidizing power of the Mars atmosphere. These continuing observations will help us constrain the long-term equilibrium of the Mars atmosphere composition. The observations presented here, covering an altitude range from the near-surface to above 110 km, provide new insights into both atmospheric dynamics and photochemistry.

Further observations will enable us to study the seasonal cycle and ratios of oxygen isotopes of CO. By incorporating data from other ACS channels and MIR grating positions, we will be able to compare CO mixing ratio profiles to simultaneous observations of aerosols and other gases, such as water vapour, ozone, and oxygen, allowing us to investigate chemical interactions, atmospheric waves or cloud interactions.

Data availability

The datasets generated by the ExoMars Trace Gas Orbiter instruments, including ACS, and analyzed during the current study are being made available in the ESA Planetary Science Archive (PSA) repository, https://archives.esac.esa.int/psa, following a six months prior access period, following the ESA Rules on Information, Data, and Intellectual Property. Data used herein can be found by searching for the "ExoMars 2016" mission and then selecting the ACS and MIR instruments. Dervied producted (CO VMR vertical profiles) have been deposited in the Oxford University Research Archive at: DOI: 10.5287/bodleian:wxxq2m6jo.

Code availability

The GGG software suite is maintained by NASA's Jet Propulsion Laboratory (JPL) and the California Institute of Technology. GGG is available at https://tccon-wiki.caltech.edu and distributed under a non-commercial software license. The LMD GCM is maintained at LMD. It can be obtained using the Subversion version control system following the instructions

made available here: https://www.lmd.jussieu.fr/~lmdz/planets/mars/user_manual.pdf

References

[1] McElroy, M. B. & Donahue, T. M. Stability of the Martian Atmosphere. *Science* **177**, 986–988 (1972).

[2] Parkinson, T. D. & Hunten, D. M. Spectroscopy and Acronomy of O_2 on Mars. *J. Atmos. Sci.* **29**, 1380–1390 (1972).

[3] Nair, H., Allen, M., Anbar, A. D., Yung, Y. L. & Clancy, R. T. A Photochemical Model of the Martian Atmosphere. *Icarus* **111**, 124–150 (1994).

[4] Yung, Y. L. & DeMore, W. B. *Photochemistry of Planetary Atmospheres* (Oxford Univ. Press, Oxford/New York, 1999).

[5] Lefèvre, F. & Krasnopolsky, V. Atmospheric photochemistry. In Haberle, R. M., Clancy, R. T., Forget, F., Smith, M. D. & Zurek, R. W. (eds.) *The Atmosphere and Climate of Mars*, Cambridge Planetary Science, 405–432 (Cambridge University Press, 2017).

[6] Krasnopolsky, V. A. Long-term spectroscopic observations of Mars using IRTF/CSHELL: Mapping of O_2 dayglow, CO, and search for CH_4. *Icarus* **190**, 93–102 (2007).

[7] Encrenaz, T. *et al.* Seasonal variations of the martian CO over Hellas as observed by OMEGA/Mars Express. *Astron. Astrophys.* **459**, 265–270 (2006).

[8] Smith, M. D., Wolff, M. J., Clancy, R. T. & Murchie, S. L. Compact Reconnaissance Imaging Spectrometer observations of water vapor and carbon monoxide. *J. Geophys. Res.* **114**, E00D03 (2009).

[9] Sindoni, G., Formisano, V. & Geminale, A. Observations of water vapour and carbon monoxide in the Martian atmosphere with the SWC of PFS/MEX. *Planet. Space Sci.* **59**, 149–162 (2011).

[10] Smith, M. D., Daerden, F., Neary, L. & Khayat, A. The climatology of carbon monoxide and water vapor on Mars as observed by CRISM and modeled by the GEM-Mars general circulation model. *Icarus* **301**, 117–131 (2018).

[11] Sprague, A. L. *et al.* Mars' south polar Ar enhancement: A tracer for south polar seasonal meridional mixing. *Science* **306**, 1364–1367 (2004).

[12] Sprague, A. L. *et al.* Interannual similarity and variation in seasonal circulation of Mars' atmospheric Ar as seen by the Gamma Ray Spectrometer on Mars Odyssey. *J. Geophys. Res.* **117**, E04005 (2012).

[13] Smith, M. D. THEMIS observations of Mars aerosol optical depth from 2002-2008. *Icarus* **202**, 444–452 (2009).

[14] Mahaffy, P. R. *et al.* Structure and composition of the neutral upper atmosphere of Mars from the MAVEN NGIMS investigation. *Geophys. Res. Lett.* **42**, 8951–8957 (2015).

[15] Stevens, M. H. *et al.* Detection of the Nitric Oxide Dayglow on Mars by MAVEN/IUVS. *J. Geophys. Res.* **124**, 1226–1237 (2019).

[16] Vandaele, A. C. *et al.* Martian dust storm impact on atmospheric H_2O and D/H observed by ExoMars Trace Gas Orbiter. *Nature* **568**, 521–525 (2019).

[17] Fedorova, A. A. *et al.* Stormy water on Mars: The distribution and saturation of atmospheric water during the dusty season. *Science* **367**, 297–300 (2020).

[18] Forget, F. *et al.* Improved general circulation models of the Martian atmosphere from the surface to above 80 km. *J. Geophys. Res.* **104**, 24155–24176 (1999).

[19] Lefèvre, F., Lebonnois, S., Montmessin, F. & Forget, F. Three-dimensional modeling of ozone on Mars. *J. Geophys. Res.* **109**, E07004 (2004).

[20] Montabone, L. *et al.* Martian Year 34 Column Dust Climatology from Mars Climate Sounder Observations: Reconstructed Maps and Model Simulations. *J. Geophys. Res.* **125**, e06111 (2020).

[21] Krasnopolsky, V. A. Variations of carbon monoxide in the martian lower atmosphere. *Icarus* **253**, 149–155 (2015).

[22] Holmes, J. A., Lewis, S. R., Patel, M. R. & Smith, M. D. Global analysis and forecasts of carbon monoxide on Mars. *Icarus* **328**, 232–245 (2019).

[23] Kass, D. M. *et al.* Mars Climate Sounder observation of Mars' 2018 global dust storm. *Geophys. Res. Lett.* **46** (2019).

[24] Smith, M. D. THEMIS Observations of the 2018 Mars Global Dust Storm. *J. Geophys. Res.* **124**, 2929–2944 (2019).

[25] Aoki, S. *et al.* Water Vapor Vertical Profiles on Mars in Dust Storms Observed by TGO/NOMAD. *J. Geophys. Res.* **124**, 3482–3497 (2019).

[26] Neary, L. *et al.* Explanation for the Increase in High-Altitude Water on Mars Observed by NOMAD During the 2018 Global Dust Storm. *Geophys. Res. Lett.* **47**, e84354 (2020).

Corresponding Author

Please address any correspondence to Dr. Kevin S. Olsen at Kevin.Olsen@physics.ox.ac.uk.

Acknowledgements

The ExoMars mission is a joint mission of the European Space Agency (ESA) and Roscosmos. The ACS experiment is led by the Space Research Institute (IKI) in Moscow, assisted by LATMOS in France. This work was funded by Roscosmos, the National Centre for Space Studies of France (CNES), the Ministry of Science and Education of Russia, the Natural Sciences and Engineering Research Council of Canada (NSERC) (PDF - 516895 - 2018), and the UK Space Agency (ST/T002069/1, ST/R001502/1 and ST/P001572/1). Science operations are funded by Roscosmos and ESA.

Author contributions

Spectral fitting of ACS MIR spectra was performed by KSO using the GGG software suite. Input and aid on spectral fitting was given by JA, CW, DB, AF, and FM. Processing of ACS spectra is done at LATMOS by LB and at IKI by AT. AF supplied ACS NIR retrievals of *P-T* profiles, and preliminary CO VMR profiles for comparison. The LMD GCM was run by FL with support from FF. The ACS instrument was operated by AT, AP, AG, and AS. All co-authors have contributed to the preparation of the manuscript, written by KSO, FL, FM and OK.

Competing interests

The authors declare no competing interests.

Figure legends

Fig. 1 | Spectral fitting with ACS MIR Example of normalized spectra recorded at 60 km with ACS MIR using secondary grating position 7. Shown are: (a) contributions from diffraction orders 250–257, (b) example fits for spectral windows covering order 252 (bottom) and the associated residuals (top).

Fig. 2 | Solar occultation latitudes Distribution over latitude and solar longitude of ACS MIR occultation using position 7, and all other ACS occultation points. The colour scale indicates the retrieved CO VMR between 20–40 km. The solar longitudes correspond to an observational period of April to September 2018.

Fig. 3 | CO VMR vertical profiles at different latitudes Vertical profiles of retrieved CO mixing ratio as observed by ACS MIR at: a) equatorial and mid-latitudes prior to Ls 190°, and b) at polar latitudes greater than ±75°. The shaded areas show the magnitude of the uncertainty of each retrieved VMR value. Lower altitude ranges are limited by signal attenuation due to aerosols. Uncertainties are derived from the non-linear least squaresd inversion using partial derivatives.

Fig. 4 | Modelled CO distributions Zonally-averaged CO volume mixing ratio (ppmv) calculated by the LMD global climate model using the MY 34 dust climatology [20] for three Ls periods: a) 165–170°, b) 180–185°, c) 210–215°. The onset of the global dust storm was around Ls 190°. The simulation shown here was initialized at Ls = 180° of MY33 and therefore avoids known issues with photochemical models underestimating the long-term equilibrium value of CO.

Fig. 5 | Time evolution of CO VMR vertical profiles Evolution of the ACS vertical profiles of CO during the MY34 dust storm. Latitudes are between −75° to 75° and colours indicate Ls.